euronoise

Coherent elastic wave propagation through non-uniform spatial distributions of cracks

Christophe Aristegui, Mihai Caleap, Olivier Poncelet, Stanislav Golkin and Alexander Shuvalov

LMP, UMR CNRS 5469, Université Bordeaux I, 351, cours de la Libération, 33405 Talence, France
c.aristegui@lmp.u-bordeaux1.fr

Models for multiple scattering of elastic waves usually concern uniform distributions of scatterers. The aim of this work is to predict the propagation of SH coherent waves through non-uniform distribution of parallel flat cracks. The spatial variation of the distribution properties is taken into account via replacing a heterogeneous medium by a stack of effective homogenous layers. Propagation in each layer is governed by the effective acoustic impedance and the effective wave number, which are derived in the framework of Waterman and Truell approach. On this basis, the reflection and transmission coefficients of the non-uniform distributions are calculated by using the transfer matrix method. We focus especially on the distribution of concentration. Impact of the distribution profiles is also investigated.

1 Introduction

Great interest in linear wave propagation through heterogeneous media, such as bubbly liquid, porous media, fiber-reinforced or/and multi-cracked composite materials, arises in many fields of physics and engineering related to investigation of material microstructure. In this context, models have been derived to predict phase velocity and attenuation of coherent plane waves [1-4].

We focus on SH coherent wave propagation in damaged medium. The energy dissipation is assumed to be due to the multiple scattering between the cracks (discontinuous phase) randomly distributed in the lossless host matrix. Significance of this study lies in considering the spatial variation of the crack density. This aspect is taken into account by replacing heterogeneous media by stacks of effective homogenous layers. Each layer is viewed as having uniform distribution with effective bulk parameters. The reflection and transmission responses of such non-uniform distribution are evaluated by using the transfer matrix method. Two approximations of the effective attenuation are also proposed.

2 Effective field parameters for uniform concentration of scatterers

We consider a linearly elastic and isotropic medium containing a random and uniform distribution of cracks. They are assumed to be identical, parallel and infinite along the axis $\boldsymbol{y}_2$. Their cross section is constant in the (y_1, y_3) plane. Ribbon-shaped (flat) cracks are represented by discontinuity lines of width $2a$ [5, 6]. The crack faces are stress-free. The number of cracks per unit area (density) is denoted by η.

An incident monochromatic SH plane wave propagates along the axis $\boldsymbol{y}_3$, normally to the crack faces. Its propagation in the lossless crack-free matrix is governed by the wavenumber $k = \omega / c_T$, where ω is the angular frequency and c_T the phase velocity of SH wave in the matrix.

It is well-known that, in presence of multiple scatterers, the coherent plane wave propagation in the two-phase (damaged) medium is described by a complex-valued wavenumber K. The losses are assumed to be induced only by the multiple scattering, i.e. the anelastic attenuation is not taken into account. For the axis adopted, the coherent wave is represented by the displacement components

$$u_1 = u_3 = 0\,,\, u_2 = A\mathrm{e}^{\mathrm{i}(Ky_3 - \omega t)}, \qquad (1)$$

where A is an amplitude factor and K is the effective wavenumber, which can be related to k in terms of the single-crack scattering amplitudes f. For brevity, the time-factor $\mathrm{e}^{-\mathrm{i}\omega t}$ is omitted in the following. In the framework of Waterman and Truell approach, we have [1, 7]

$$K^2 = k^2\left(1 + \eta\frac{2\pi}{k^2}f(0)\right)^2 - k^2\left(\eta\frac{2\pi}{k^2}f(\pi)\right)^2, \qquad (2)$$

where $f(0)$ and $f(\pi)$ stand for the far-field amplitudes scattered by a single object in the forward and backward directions. In the special case of flat cracks, the expression for the amplitudes f may be found in Ref. [8].

Alternatively, the dynamic mechanical behavior of a two-phase medium subjected to multiple scattering of SH waves can be described macroscopically. Due to symmetry of cracks and their uniform and parallel arrangement, the damaged medium behaves as an orthotropic homogeneous medium. We have expressed the effective mass density, and the effective shear stiffness along the axis $\boldsymbol{y}_3$ as [9]

$$\rho = \rho_0\left(1 + \frac{2\pi\eta}{k^2}\big(f(0) + f(\pi)\big)\right), \qquad (3)$$

$$M = \mu_0\left(1 + \frac{2\pi\eta}{k^2}\big(f(0) - f(\pi)\big)\right)^{-1}, \qquad (4)$$

with ρ_0 and μ_0 standing for the mass density and the stiffness of the matrix. The effective acoustic impedance

$$Z = \rho\omega / K\,, \qquad (5)$$

can then be calculated from Eqs. (2) and (3). Note that the complex-valued bulk parameters ρ and M depend on the frequency and the crack density η.

3 Transfer matrix method

Consider a multilayered medium of thickness h, embedded in the matrix defined in Sec. 2, Fig. 1. Each of the p parallel layers is characterized by a wavenumber k_j, a shear stiffness μ_j and a constant thickness $d_j = h / p$. The lateral dimensions of the layers are assumed to be infinite. The multilayered stack is subjected to a SH plane wave normally incident on the first layer. The outcoming waves are evaluated at the exit of the last layer. The surrounding matrix is assumed in the form of semi-infinite substrates and bounded on both sides of the multilayered medium.

Introduce the SH state vector $\boldsymbol{W}$,

$$\boldsymbol{W}(y_3) = \begin{bmatrix} u_2(y_3) \\ \sigma_{23}(y_3) \end{bmatrix}, \qquad (6)$$

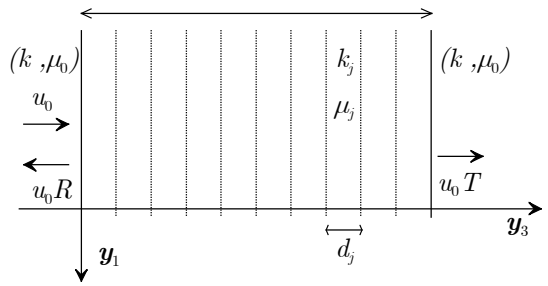

Fig.1 Schematic representation of a multilayered medium, such as $h = \sum_j d_j$.

composed by the out-of-plane displacement u_2 and the shear stress component σ_{23}. The state vectors at both faces of each layer can be related as follows

$$\boldsymbol{W}\left(\xi_{j+1}\right) = m_j\left(\omega, k_j, \mu_j, d_j\right)\boldsymbol{W}\left(\xi_j\right), \tag{7}$$

where $m_j\left(\omega, k_j, \mu_j, d_j\right) = \begin{bmatrix} \cos k_j d_j & \dfrac{\sin k_j d_j}{k_j \mu_j} \\ -k_j \mu_j \sin k_j d_j & \cos k_j d_j \end{bmatrix}$, (8)

and where $y_3 = \xi_j$ is the upper interface of the j^{th} layer. Invoking the continuity of the state vector (6) at the interfaces between the layers, the state vectors at both edges of the multilayered medium, $y_3 = 0$ and $y_3 = h$, are related as follows

$$\boldsymbol{W}(h) = m(\omega)\boldsymbol{W}(0), \tag{9}$$

where $$m(\omega) = \prod_{j=p}^{1} m_j\left(\omega, k_j, \mu_j, d_j\right), \tag{10}$$

is the transfer matrix through the layers [10].

We now consider the wave fields outside the multilayered medium. The incident wave of amplitude u_0 and wavenumber k is reflected by the first interface (amplitude R) and transmitted through the stack of layers (amplitude T). The state vectors $\boldsymbol{W}(0)$ and $\boldsymbol{W}(h)$ are written as

$$\boldsymbol{W}(h) = u_0 \begin{bmatrix} T\mathrm{e}^{\mathrm{i}kh} \\ \mathrm{i}k\mu_0 T\mathrm{e}^{\mathrm{i}kh} \end{bmatrix} \text{ and } \boldsymbol{W}(0) = u_0 \begin{bmatrix} 1+R \\ \mathrm{i}k\mu_0(1-R) \end{bmatrix}. \tag{11}$$

where $\mu_0 = \rho_0 c_T^2$. Thus, the two unknown amplitudes R and T are evaluated from the system of two equations established by combining Eqs. (7)-(11).

The above-outlined transfer matrix method is applied to damaged layers subjected to multiple scattering between cracks. Each multi-cracked layer is replaced by an appropriate effective homogenous layer. The surrounding medium is the matrix. The dynamic behavior of each damaged layer containing η_j cracks per unit area, is governed by the effective wavenumber $K_j\left(\eta_j\right)$ and the effective shear stiffness $M_j\left(\eta_j\right)$, $j = 1 \ldots p$, see Eqs. (2) and (4). The reflection and transmission responses of the stack of damaged layers are then evaluated from Eqs. (9) and (11), in which the parameters k_j and μ_j are replaced by $K_j\left(\eta_j\right)$ and $M_j\left(\eta_j\right)$. The matrix m in Eq. (9) becomes

$$m\left(\omega, \eta(y_3)\right) = \prod_{j=p}^{1} m_j\left(\omega, K_j\left(\eta_j\right), M_j\left(\eta_j\right), d_j\right), \tag{12}$$

where $\eta(y_3)$ stands for the spatial function of the crack density over the multilayer depth.

4 Application to non-uniform concentration of cracks

The non-uniform crack density $\eta(y_3)$ of parallel identical flat cracks is introduced by replacing multi-cracked media by stacks of effective homogenous layers with a constant crack density η_j each.

Numerical results are obtained for the space-varying crack density

$$\eta(y_3) = \eta_0 \frac{\mathrm{e}^{-\left(\frac{y_3 - h/2}{\sigma}\right)^2} - \mathrm{e}^{-\left(\frac{h/2}{\sigma}\right)^2}}{1 - \mathrm{e}^{-\left(\frac{h/2}{\sigma}\right)^2}}, \tag{13}$$

for $0 \le y_3 \le h$ (so that $\eta(0) = \eta(h) = 0$), with $\sigma = 0.005$, $h = 30.3\ mm$ and $a = 1\ mm$, see Fig. 2. The maximum value of Eq. (13) is taken as $\eta(h/2) = 30\,000$ cracks$/m^2$. The matrix material is aluminum with $c_T = 3.13\ m/ms$ and $\rho_0 = 2.7\ g/cm^3$.

4.1 Effect of the discretization

The non-uniform multi-cracked medium is viewed as p layers of thickness $d_j = d = h/p$. The moduli of the reflection and transmission coefficients are shown in Fig. 3 as functions of the frequency ν for several values of p. Note that the dimensionless frequency $\tilde{\omega} = ka$ is less than 6 when ν is less than 3 MHz. The amplitude of $|R|$ is displayed in the logarithm scale in all the figures.

When the number of layers increases, the values of the crack density at the first and last layers decrease and approach zero. Therefore, the difference between the acoustic impedance of the matrix and those of the 1^{st} and p^{th} tends to zero. While the transmission coefficient is independent of the layer number, some artifacts appear in $|R|$ for frequencies $\nu^{(q)}$ corresponding to the resonances of a single layer. They can be approximated from the wavelength λ of the incident wave, as follows

$$d_j \approx q\frac{\lambda}{2} \Leftrightarrow \nu^{(q)} \approx q\frac{pc_T}{2h}, \tag{14}$$

where $q = 1, 2 \ldots$. When the number of layers increases, the resonance frequencies move to higher frequency and, therefore, depart from the plots. In the following, p is chosen to be equal to 101.

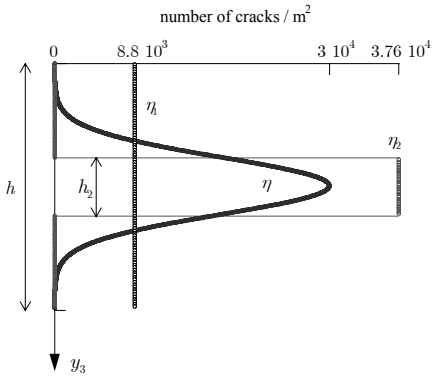

Fig.2 Profiles of crack density. $\eta(y_3)$ is given by Eq. (13), while $\eta_1(y_3)$ and $\eta_2(y_3)$ satisfy Eq. (15).

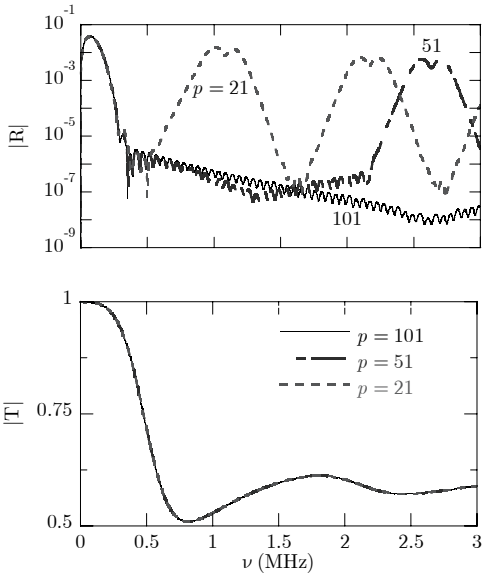

Fig.3 Moduli of the reflection and transmission coefficients for the space-varying crack density (13). The number of layers takes values $p = 21, 51, 101$.

4.2 Different profiles of concentration

In this section, we introduce two additional uniform crack densities, $\eta_1(y_3) = \eta_1$ and $\eta_2(y_3) = \eta_2$, which have the same number of cracks as that of the Gaussian profile (13), over the range $[0, h]$, see Fig. 2. Thus, their mean values are all identical, according to

$$\frac{1}{h}\int_0^h \eta(y_3)dy_3 = \eta_1 = \eta_2 \frac{h_2}{h}. \qquad (15)$$

While the depth of $\eta_1(y_3) = \eta_1$ is h, the depth of $\eta_2(y_3) = \eta_2$ is chosen such as $h_2 = \sqrt{2}\sigma$. This value corresponds to the distance between the coordinates y_3, where the variation of the profile $\eta(y_3)$ is the highest.

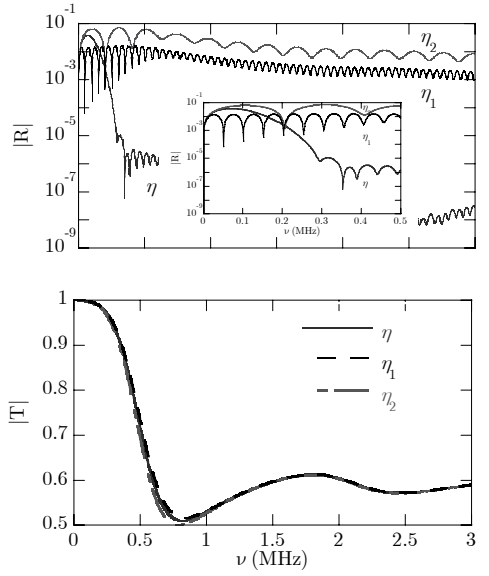

Fig.4 Moduli of the reflection and transmission coefficients for the three profiles of crack density displayed in Fig. 2. The low-frequency part of $|R|$ is zoomed.

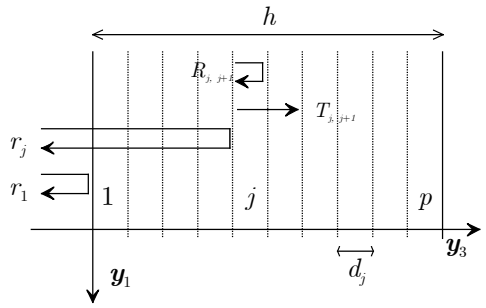

Fig.5 Partial wave decomposition. Exchanges between two successive layers, j^{th} and $(j+1)^{th}$: $R_{j,j+1}, T_{j,j+1}$. Specular reflection by the j^{th} interface: r_j .

The reflection and transmission coefficients calculated for each of the three space-varying crack densities coincide at very low frequency, Fig. 4. Indeed, the incident wave interferes with the same number of cracks.

4.3 Partial wave decomposition

Individual reflection and transmission coefficients at an interface between the j^{th} and $(j+1)^{th}$ layers are given by

$$R_{j,j+1} = \frac{z_j - z_{j+1}}{z_j + z_{j+1}} \text{ and } T_{j,j+1} = \frac{2z_j}{z_j + z_{j+1}}, \qquad (16)$$

where z_j stands for the acoustic impedance of the j^{th} layers, Fig. 5. In the special case of multi-cracked layers, z_j depends on the crack density η_j and, then, are evaluated from Eq. (5). The coefficients (16) are used in the Debye serie method of calculating the aggregate reflection and transmission coefficients.

In this context, the spectrum of the forward propagating wave through the first $(j-1)^{th}$ layers, reflected by the j^{th} interface and going back towards the matrix, Fig. 5, can be expressed as

$$\begin{cases} r_1 = R_{0,1} \\ r_j = R_{j-1,j} e^{2i\sum_{q=1}^{j-1} K_q(\eta_q) d_q} \prod_{q=1}^{j-1} T_{q-1,q} T_{q,q-1}, \quad 2 \le j \le p+1 \end{cases} \qquad (17)$$

with $R_{p,p+1} = R_{p,0}$. The properties of the surrounding matrix are indicated by the subscript 0.

Fig. 6 shows a comparison between the reflection coefficient R of the multilayered medium and the sum of the specular reflection (17) by all the $p+1$ interfaces. A good agreement between these predictions outlines that the reverberations inside each single layer are negligible.

The effect of the internal reverberations on $|T|$ is now investigated by taking into account only the propagation over each layer. Fig. 6 compares $|T|$ and

$$\left| \exp\left(i\sum_{j=1}^{p} K_j(\eta_j) d_j \right) \right|. \qquad (18)$$

The two curves match well. The internal reverberations still remain insignificant for the calculation of T .

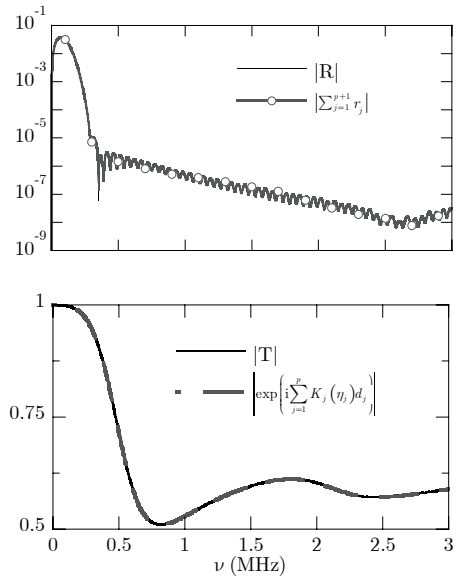

Fig.6 Moduli of the reflection and transmission coefficients for the space-varying crack density (13). Approximation obtained by neglecting the reverberations inside each single layer: (a) $\left|\sum_{j=1}^{p+1} r_j\right|$, with Eq. (17); (b) Eq. (18).

4.4 Effective attenuation: approximation

For the density profile (13), we assess the effective attenuation α of the multilayered medium from the transmission coefficient T evaluated by using the transfer matrix method described in Sec. 2. Neglecting the difference in the acoustic impedances between the matrix and the damaged region, we have $\mathrm{e}^{-\alpha h} \approx |T|$, and so,

$$\alpha \approx -\frac{\log T}{h}. \tag{19}$$

Discarding the reverberation between the layers (thereby disregarding the non-uniformity of the crack density, see Sec. 4.3), the effective attenuation can also be evaluated from

$$\alpha \approx \frac{1}{p}\sum_{j=1}^{p} \mathrm{Im}\, K_j\left(\eta_j\right), \tag{20}$$

where the effective wavenumber of the j^{th} layer is given by Eq. (2).

Fig. 7 shows the effective attenuation (19) and (20) of the coherent plane wave propagating through the non-uniform density of crack $\eta(y_3)$. The two curves coincide because the reverberation has been discarded.

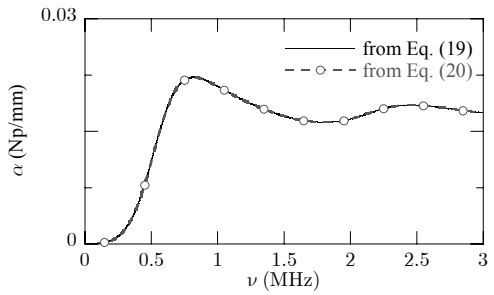

Fig.7 Approximations (19) and (20) of the effective attenuation of the coherent wave propagating through the profile of space-varying crack density (13).

5 Summary

We have investigated SH coherent wave propagation in space-varying distribution of parallel flat cracks embedded in an elastic matrix. The non-uniform distribution is approximated by a stack of layers each with a uniform distribution.

The resonance frequencies of the individual layers have been shown to affect the reflection response of the multilayered medium.

At low frequency, the response of the Gaussian distribution coincides with that of constant distributions of appropriate value and depth.

The effects of the reverberations inside each layer on the reflection R and transmission T coefficients of the non-uniform distribution are negligible for the case studied.

References

[1] P. C. Waterman and R. Truell, "Multiple scattering of waves," *J. Math. Phys.*, 2, 512-537 (1961).

[2] Y. C. Angel and Y. K. Koba, "Complex-valued wavenumber, reflection and transmission in an elastic solid containing a cracked slab region," *Int. J. Solids Struct.*, 35, 573-592 (1998).

[3] C. M. Linton and P. A. Martin, "Multiple scattering by random configurations of circular cylinders: Second-order corrections for the effective wavenumber," *J. Acoust. Soc. Am.*, 117, 3413-3423 (2005).

[4] S. Robert and J.-M. Conoir, "Reflection and transmission process from a slab-like region containing a random distribution of cylindrical scatterers in an elastic matrix," *Acustica*, 93, 1-12 (2007).

[5] P. M. Morse and P. J. Rubenstein, "The diffraction of waves by ribbons and by slits," *Phys. Rev.*, 54, 895-898 (1938).

[6] Y. C. Angel, "On the reduction of elastodynamic crack problems to singular integral equations," Int. J. Eng. Sci., 26, 757-764 (1988).

[7] M. Caleap, C. Aristégui and Y. C. Angel, "Comparing two approaches for multiple scattering: line-like or actual size scatterers," presented at the 4th Journées du GDR CNRS 2501, Giens, France, 14-19 May, 2006, 254-262, Ed. INRIA (Le Chesnay, France), ISBN 2-7261-1282-x (2007).

[8] M. Caleap, C. Aristégui and Y. C. Angel, "Further results for antiplane scattering by a thin strip," *J. Acoust. Soc. Am.*, 122, 1876-1879 (2007).

[9] C. Aristégui and Y. C. Angel, "Effective material properties for shear-horizontal acoustic waves in fiber composites," *Phys. Rev. E*, 75, 056607 (2007).

[10] A. L. Shuvalov, O. Poncelet and M. Deschamps, "General formalism for plane guided waves in transversely inhomogeneous anisotropic plates," *Wave Motion*, 40, 413-426 (2004).